Available online at www.sciencedirect.com
SCIENCE DIRECT®
Journal of Organometallic Chemistry 675 (2003) 57–64
Journal of Organometallic Chemistry
www.elsevier.com/locate/jorganchem

Rhenium carbonyl complexes of 2,6-diazaanthracene-9,10-dione(daad): spectroelectrochemistry of $BrRe(CO)_4daad$

Joy L. Morgan *, Amar H. Flood, Keith C. Gordon, Brian H. Robinson *, Jim Simpson

Department of Chemistry, University of Otago, P.O. Box 56, Dunedin, New Zealand

Received 26 February 2003; received in revised form 27 March 2003; accepted 28 March 2003

Abstract

An analysis of the X-ray structure, vibrational and electronic spectra of $BrRe(CO)_4daad$, **2**, and a spectroscopic study of the radical anion $\mathbf{2}^{\bullet -}$ are presented (daad = 2,6-diazaanthracene-9,10-dione). Strong π-stacking is seen in the crystal structure of **2**. Electronic absorption, resonance Raman vibrational analysis and electrochemistry of **2** support an assignment of the HOMO and LUMO to a predominately metal dπ and ligand π* orbital (localised on the quinoidal ring), respectively. There is poor orbital overlap between donor Re (dπ) and acceptor ligand π* MOs. **2** undergoes a ligand-based reduction process at −0.24 V vs. decamethylferrocene to give $\mathbf{2}^{\bullet -}$ which was investigated by spectroelectrochemistry and isolated as the $[Cp_2Co]^+$ salt. Insoluble $[XRe(CO)_3daad]_n$ and unstable $XRe(CO)_3(daad)_2$ complexes, where X = Br or Cl, were also identified.

Keywords: Azaquinone; Rhenium carbonyl complexes; Radical anion; X-ray structure; Spectroelectrochemistry

1. Introduction

Multicomponent emissive molecular assemblages which incorporate transition metal ions are the subject of extensive research, particularly where precisely positioned long-range and short-range interactions drive self-organisational processes to maintain structural integrity [1,2]. This area is dominated by a functional design focus on solution-phase recognition and binding properties of substrates for chemical sensing, catalysis and biomimetric intramolecular charge transfer [3]. These solution-phase concepts have been extended to thin films and mesoporous structures [4]. Assemblages with coupled redox-active organometallic components and organic fluorophores [5] are not so well explored. A problem with this type of assemblage is the accessibility of emissive decay mechanisms which lead to decreased emission from the organic chromophores [6]. As part of a study, aimed at elucidating the parameters which can ameliorate energy transfer in this type of emissive redox-switchable assemblage, we have investigated complexes of the difunctional azaquinone, 2,6-diazaanthracene-9,10-dione (daad) **1**, with rhenium(I) carbonyl units.

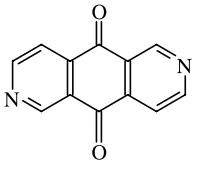

1

Molecular squares of Pd(II) and Pt(II) [7,8] using **1** as the cornerstone are well-known and square assemblies range in cavity size from < 5 Å to > 30 Å. Considerable effort has been devoted to improving selectivity and sensitivity of molecular recognition [7], optical activity [9] and photoluminescence [10] of these heavy-metal squares. An $XRe(CO)_n$ unit, where X = Br, Cl or the redox moiety ferrocenyl, was chosen as the acceptor for our study as their complexes with polypyridyl ligands have a single chromophore and usually an unambiguous site of electron localisation when reduced [11,12]. The redox and spectroscopic properties of the monomer $BrRe(CO)_4daad$ are described herein. Other complexes of Re(I) and daad proved to be extremely labile and unexpectedly strong intramolecular interactions pre-

* Corresponding authors. Fax: +64-3-479-7906.
E-mail address: joy@alkali.otago.ac.nz (J.L. Morgan).

0022-328X/03/$ - see front matter © 2003 Elsevier Science B.V. All rights reserved.
doi:10.1016/S0022-328X(03)00231-6

vented the development of a series of soluble extended arrays, the thermodynamic products being insoluble $[XRe(CO)_3daad]_n$.

2. Results and discussion

The reaction of $BrRe(CO)_5$ with **1** proceeds through several stages summarized in Scheme 1 and the product mix is determined by the temperature and solvent used for the reaction.

In boiling hexane, $BrRe(CO)_5$ and **1** gave sequentially the soluble monomer building block **2**, the corner building block of a square, **3** and insoluble **4**; at room temperature, in dichloromethane in the presence of acetonitrile and Me_3NO, a mixture of **2**, **3** and **4** was produced. No reaction took place between $BrRe(CO)_5$ and **1** in dichloromethane at 40 °C. Reactions carried out in a more polar solvent or at a higher temperature gave only an insoluble orange powder **4**, which is the ultimate product when handling solutions of **2** and **3**.

2 was very labile and it was difficult to obtain pure samples for microanalysis without contamination from **1** and **4** but it was able to be characterised by FABMS, a X-ray crystal structure and spectroscopic measurements. The IR ν(ReCO) profile at 2115, 2016, 2004 (sh), 1943 is typical of a $Re(CO)_4$ unit bound to an *N*-donor [13], with the presence of the mode at 2115 cm^{-1} distinguishing $Re(CO)_4$ from $Re(CO)_3$ complexes. The ligand ν(C=O) at 1696 cm^{-1} compared to 1686 cm^{-1} for **1** shows that complexation leaves the quinoidal framework unperturbed. Coordination of $Re(CO)_4$ causes a down-field shift of the ^1H and ^{13}C aromatic resonances in the aza ring system directly bound to the Re, thus assisting in the assignment. The asymmetric profile of the ligand ^1H and ^{13}C resonances are consistent with coordination of one nitrogen donor per $BrRe(CO)_4$ unit.

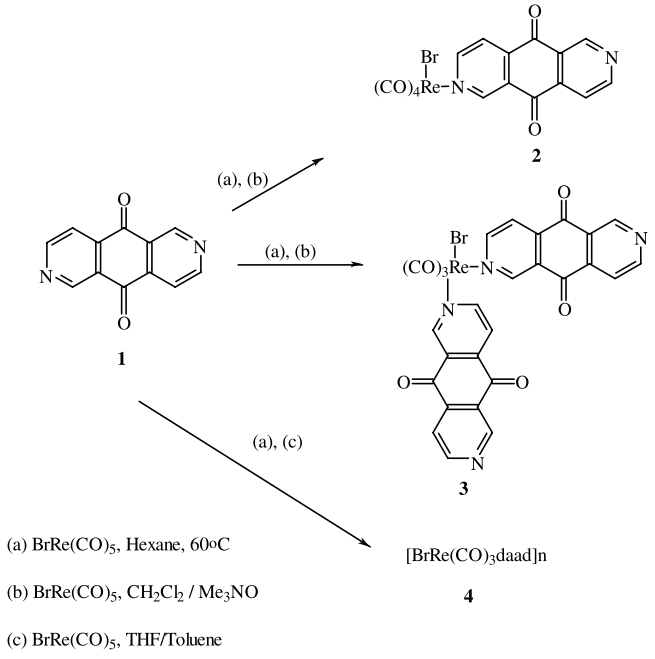

Scheme 1.

A perspective view of **2** is shown in Fig. 1 and defines the atom numbering scheme for the crystal structure and NMR of **2**. Crystals of **2** contain discrete molecules, the shortest intermolecular distance (not involving H atoms) being 2.897 Å C(8)···O(14), $(x, 3/2-y, (1/2)+z)$. Table 1 lists selected bond lengths and angles. Coordination at the Re atom is approximately octahedral with the diazaanthraquinone ligand *cis* to the bromine substituent (Fig. 1). There is only one reported X-ray structure of a rhenium complex with an equivalent donor set and orientation, viz *cis*-bromo-tetracarbonyl(2-(4-pyridyl)ethenylferrocene-rhenium [14]. The diazaanthraquinone ligand adopts a staggered orientation with respect to the ligands in the equatorial plane with interplanar angles of 37.0(2)° (to Re(1) C(21) C(22) C(23)) and 54.8(2)° (to Re(1) Br(1) C(21) C(24)), respectively, suggesting that the minimization of steric interactions is important in determining the solid state structure. The ligand is also inclined at an angle of 80.17(9)° to the (Re(1) Br(1) C(22) C(23) C(24) plane. Coordination to rhenium results in a slight deformation of the diazaanthraquinone. The angle between the planes of the coordinated heterocyclic and the quinoidal rings increased to 4.7(3)° from 0.80(7) and 1.07(6)°, respectively, for the two individual molecules in the unit cell of **1** [15]. Otherwise, bond distances and angles are similar to those observed in the corresponding rings of **1** [15] and the three other reported azaanthraquinone structures [16]. The Re–Br and Re–N bond distances are similar to those found in other bromo and pyridyl substituted rhenium carbonyls [17], and in the parent $BrRe(CO)_5$ [18]. π-Stacking also contributes significantly to the stabilisation of the solid state structure of **2**, although this is reduced in comparison to the extended interactions observed for the uncomplexed ligand, **1** [15]. Strong π-stacking interactions are observed between adjacent pairs of daad ligands, arranged in a head-to-tail fashion along the *z*-axis (Fig. 2). The head-to-tail arrangement ensures that the bulky $BrRe(CO)_4$ moieties can pack in an unimpeded fashion at opposite ends of the stacked daad ligand pairs. Centroid–centroid distances between the ligands are in the range 3.78–3.80 Å, only slightly longer than those in **1** (3.67–3.77 Å) [15]. However, the angles between the ring normals and the centroid–centroid vectors, 26.3–30.9°, are larger than those for **1** (20.8–26.4°) [15] indicating that there is a greater ring slippage or offset orientation in **2**.

The corner building block for a square, **3**, was characterised by microanalysis and spectroscopy. The ν(CO) profile of 2033, 1939, 1902 (Re–CO) and 1695

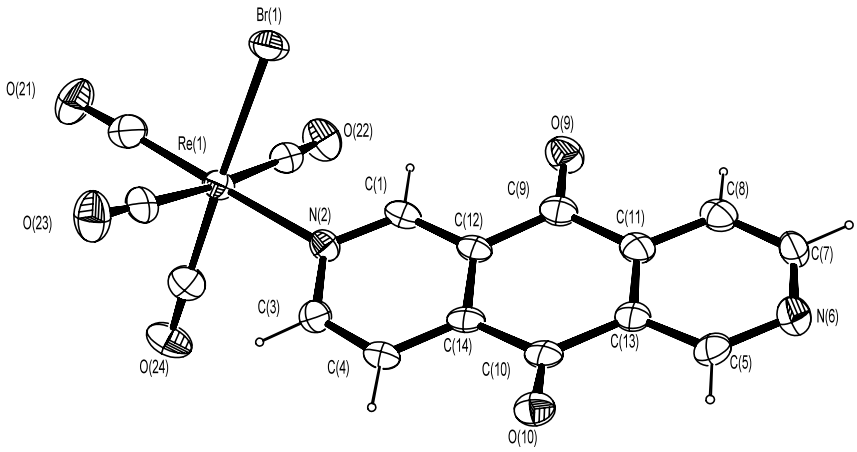

Fig. 1. Perspective view of **2** showing the atom numbering scheme, with displacement ellipsoids drawn at the 50% probability level.

Table 1
Selected bond lengths (Å) and angles (°) for **2**

Re(1)–Br(1)	2.6168(11)	C(7)–C(15)	1.401(7)
Re(1)–C(1)	1.938(8)	C(7)–C(8)	1.496(8)
C(1)–O(1)	1.151(8)	C(8)–O(8)	1.224(6)
Re(1)–C(2)	1.988(8)	C(8)–C(9)	1.508(8)
C(2)–O(2)	1.159(8)	C(9)–C(10)	1.392(8)
Re(1)–C(3)	1.910(7)	C(9)–C(13)	1.397(7)
C(3)–O(3)	1.159(8)	C(10)–N(2)	1.345(7)
Re(1)–C(4)	2.010(8)	N(2)–C(11)	1.333(8)
C(4)–O(4)	1.149(8)	C(11)–C(12)	1.385(8)
Re(1)–N(1)	2.212(5)	C(12)–C(13)	1.398(8)
N(1)–C(5)	1.356(6)	C(13)–C(14)	1.499(8)
N(1)–C(16)	1.342(7)	C(14)–O(14)	1.218(6)
C(5)–C(6)	1.366(7)	C(14)–C(15)	1.488(8)
C(6)–C(7)	1.404(7)	C(15)–C(16)	1.379(8)
N(1)–Re(1)–Br(1)	85.11(13)	C(3)–Re(1)–C(2)	90.2(2)
C(1)–Re(1)–Br(1)	92.9(2)	C(3)–Re(1)–C(4)	93.6(2)
C(1)–Re(1)–N(1)	177.3(2)	C(3)–Re(1)–N(1)	93.3(2)
C(1)–Re(1)–C(2)	89.1(2)	C(4)–Re(1)–N(1)	89.62(18)
C(1)–Re(1)–C(4)	88.4(2)	C(3)–Re(1)–Br(1)	178.2(2)
C(2)–Re(1)–C(4)	175.4(2)	C(2)–Re(1)–Br(1)	89.04(14)
C(2)–Re(1)–N(1)	92.75(17)	C(4)–Re(1)–Br(1)	87.29(15)
C(3)–Re(1)–C(1)	88.7(3)		

(daad) cm^{-1} and the asymmetric ligand ^{1}H and ^{13}C-NMR resonances were consistent with a $BrRe(CO)_3$ moiety coordinated to two ligand molecules [13]. The microanalytical and spectroscopic data for the insoluble product **4** were compatible with $[BrRe(CO)_3daad]_n$ but its insolubility precluded NMR measurements and FABMS or ESMS were inconclusive. A number of different approaches were tried, unsuccessfully, to solubilise $[BrRe(CO)_3daad]_n$. These included reactions with the ferrocenium species $[FcRe(CO)_5]^+$ and reactions with $Cp_2Co^+\mathbf{2}^{\bullet -}$ where it was thought that the effect of the charged species might reduce the intermolecular interactions causing the insolubility.

$ClRe(CO)_5$ reacted more rapidly with **1** and while comparable intermediates to **2** and **3** could be detected only $ClRe(CO)_3daad_2$ was characterised spectroscopically. Essentially, insoluble complexes similar to **4** were the ubiquitous result [19] of any reaction of **1** with $ClRe(CO)_5$ or $FcRe(CO)_5$.

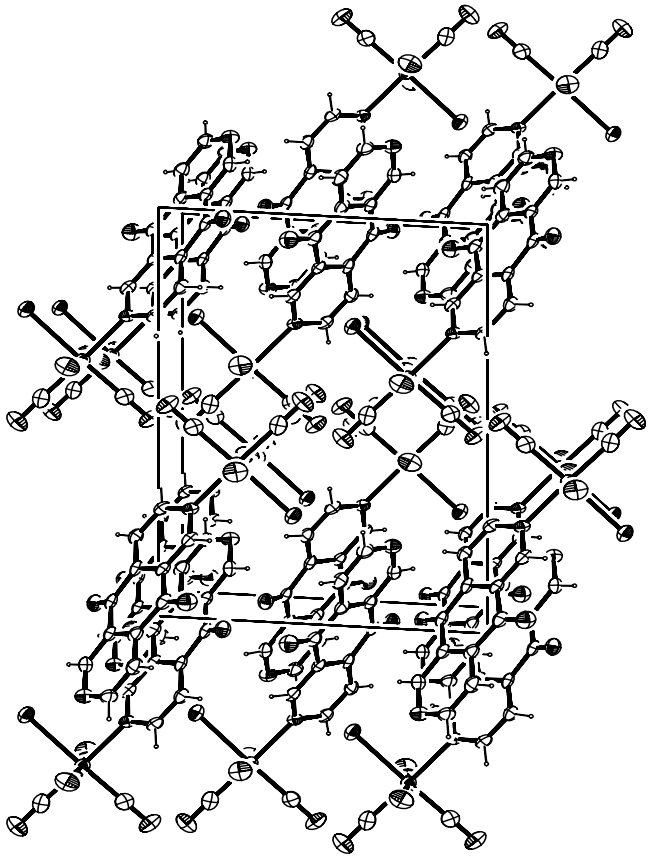

Fig. 2. Packing diagram of **2**.

2.1. Electronic and vibrational spectroscopy of *2*

For chelated {$XRe(CO)_3$polypyridyl} complexes the HOMO is usually a dπ MO of the Re(I) center and the

LUMO a ligand-based π* MO [12,20]. The metal and ligand π orbitals may be electronically coupled by dπ–π* back bonding which has a role in determining the energy- and electron-transfer properties of the rhenium complex [21]. The structural and spectroscopic data herein for **2** and its radical anion $\mathbf{2}^{\bullet -}$ indicate that there is only weak coupling in complexes with daad.

The lowest energy band in the electronic spectrum of the ligand **1**, observed at 317 nm ($\varepsilon = 4700\ M^{-1}\ cm^{-1}$) in dichloromethane, is a transition from an energy level from configurationally mixed orbitals below the HOMO to the LUMO (b_g); the HOMO (a_g)—LUMO transition is symmetry forbidden [15]. This band is unperturbed by coordination to the $Re(CO)_4$ unit, occurring at 316 nm ($\varepsilon = 5900\ M^{-1}\ cm^{-1}$) in **2** (Table 2). For complex **2** a new band at lower energy occurs at 431 nm ($\varepsilon = 300\ M^{-1}\ cm^{-1}$) and is assigned to a $Re(d\pi) \rightarrow 1(\pi^*)$ MLCT transition. This assignment aligns with those for MLCT transitions observed for $\{XRe(CO)_3(N–N)\}$ complexes [22] although typically, the chelated complexes tend to be of lower energy than that for **2** and their intensity is usually $\gg 1000\ M^{-1}\ cm^{-1}$. Complexation stabilises the ligand-based LUMO and both the higher energy and the very weak intensity of the MLCT transition for **2** reinforces the view that this stabilisation is not as effective as for polypyridyl ligands; the dπ–π* coupling is weak. Furthermore, the smaller stabilisation with **1** as a ligand is consistent with the lower amplitude of the acceptor orbital of the coordinating nitrogen atom, C_N^2 (0.04), as obtained from B3LYP DFT calculations [15] compared with the typical value of 0.1–0.2 per nitrogen donor for polypyridyl complexes [20e,20g].

The skeletal ring mode at 1612 cm^{-1} in **1** is shifted to 1579 cm^{-1} in **2** upon coordination (Table 2). The resonance Raman spectrum ($\lambda_{exc} = 457.9$ nm) of **2** (Fig. 3) shows strong enhancement of the 2114 cm^{-1} ν(ReCO) mode and the 1691 and 1612 cm^{-1} ligand modes which conclusively supports the MLCT band assignment and the premise that bonding of the acceptor results in perturbation of the quinoidal ligand orbital [12].

2.2. Spectroelectrochemistry of 2

Cyclic and square wave voltammetry of **2** in CH_2Cl_2 display a kinetically slow ($\Delta E = 130$ mV) and chemically reversible ($i_p/i_a = 1$) one-electron reduction to the radical anion at −0.24 V vs. decamethylferrocene (cf. −0.49 V for 1). A second, partially reversible, reduction step follows at $E_c = -1.10$ V; there are no oxidation processes in the range 0.00–1.00 V. Normally, the decrease in $E^{0/-1}$ for non-quinoidal, chelating ligands on complexation to rhenium is ca. 800 mV [23] and there is a clear correlation between $E^{0/-1}$, the lowest energy (MLCT) transition and the degree of dπ–π* coupling [19]. It is significant that the decrease in $E^{0/-1}$ upon daad coordination (250 mV) is much smaller than these typical values for polypyridyl complexes, indicative of weak dπ–π* coupling between the donor and acceptor.

Chemical reduction of **2** with cobaltocene in benzene gave $[Cp_2Co]^+$ $\mathbf{2}^{\bullet -}$ as a dark blue unstable solid. Its spectroscopic properties were identical to $\mathbf{2}^{\bullet -}$ generated by controlled potential reduction of **2** at −0.3 V vs. decamethylferrocene and in situ OTTLE spectroelectrochemistry [24]. B3LYP/6-31G calculations indicate that the singly occupied molecular orbital (SOMO) of $\mathbf{1}^{\bullet -}$ is similar to the LUMO of **1** [15]. Thus, the major spectroscopic consequences of reduction to $\mathbf{1}^{\bullet -}$ as in $\mathbf{2}^{\bullet -}$ should be seen in the vibrational spectra of the quinoidal ring.

A series of IR OTTLE spectra of **2** upon electrochemical reduction is shown in Fig. 4. The daad ligand modes of $\mathbf{2}^{\bullet -}$ in the 1700–1500 cm^{-1} region are similar to those of $\mathbf{1}^{\bullet -}$ [15]. Electrochemical reduction of **2** results in bleaching of the 1696 cm^{-1} band concomitant with the growth of a new feature at 1514 cm^{-1}. This new band corresponds to an asymmetric stretch of the ring system; the comparable modes for $\mathbf{1}^{\bullet -}$ [15] and the 9,10-anthraquinone radical anion [25] are 1509 and 1496 cm^{-1}, respectively. The large shift in this asymmetric mode upon reduction, $\Delta\nu = -190\ cm^{-1}$ is consistent with the calculated LUMO nodal structure and the large wavefunction amplitude at the quinoidal portion of the

Table 2
Spectroscopic data

	UV–vis [a] λ_{max} (nm) ($\varepsilon \times 10^{-2}$ ($l\ mol^{-1}\ cm^{-1}$))	IR [a] ν(Re–CO) (cm^{-1})	IR [a] ν(daad) (cm^{-1})	Resonance Raman [a] ν(cm^{-1})
1	317 (*47*)	–	1686, 1579	1679, 1593
$\mathbf{1}^{\bullet -}$	403 (*47*), 573 (*68*), 909 (*11*)	–	1581, 1509	–
2	316 (*59*), 431 (*3*)	2115, 2016, 2004 (sh), 1943	1696, 1587	2114, 2032, 2000, 1942, 1691, 1612, 1587 [b]
$\mathbf{2}^{\bullet -}$	267 (*121*), 387 (*37*), 620 (*62*), 985 (*3*)	2110, 2010, 1935	1612, 1514	2111, 1688, 1616, 1576 [b], 1734, 1619, 1577 [c]

[a] In CH_2Cl_2 at 20 °C; TBAP, Pt, 0.1 mol l^{-1}.
[b] 457.9 nm excitation.
[c] 514.5 nm excitation.

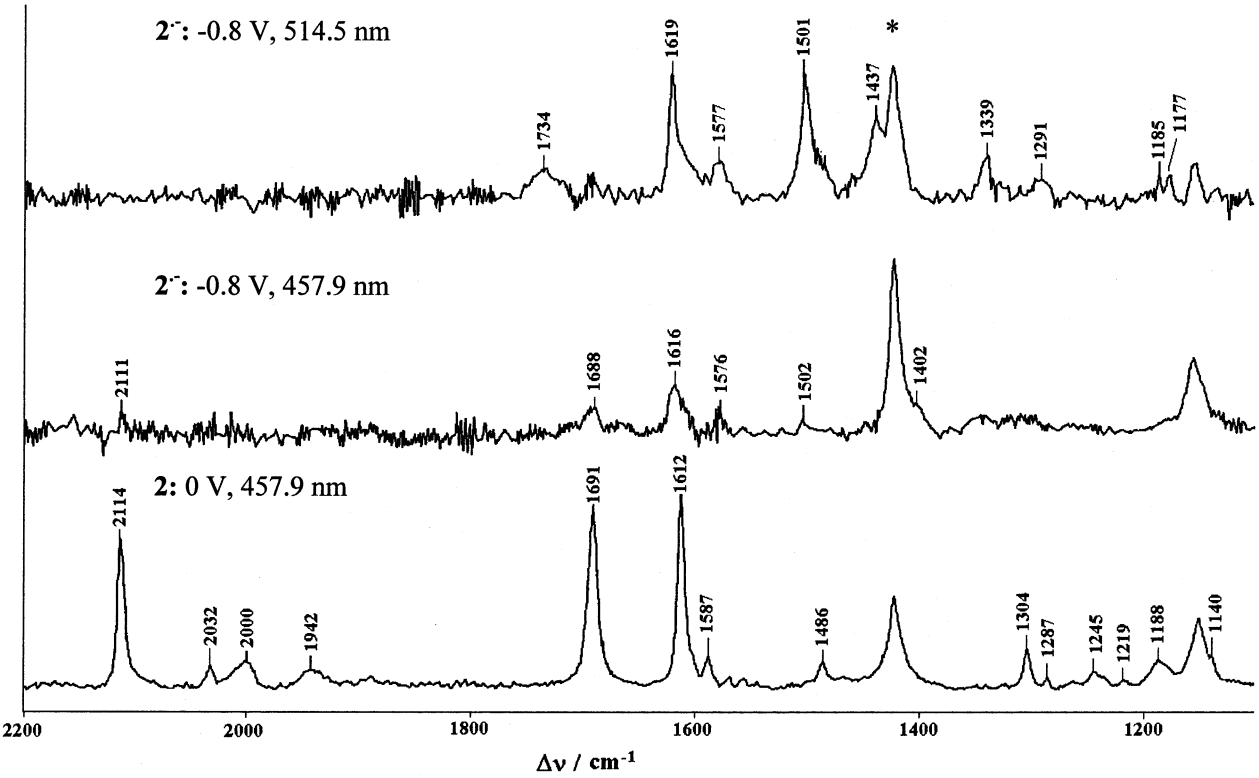

Fig. 3. Resonance Raman spectrum of **2** and $\mathbf{2}^{\bullet -}$ at different excitation wavelengths, in CH_2Cl_2; Pt electrode, TBAP, 0.1 mol l^{-1}. * Denotes solvent feature.

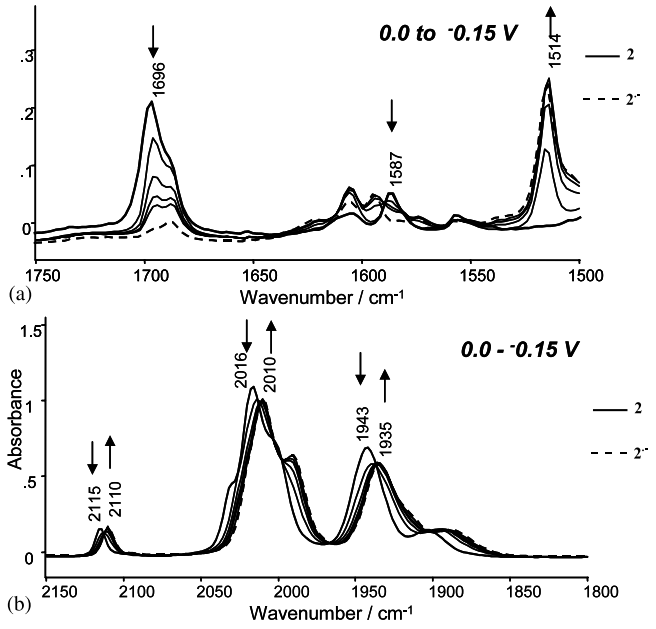

Fig. 4. IR vibrational spectroelectrochemistry of **2** being reduced to $\mathbf{2}^{\bullet -}$ in CH_2Cl_2; Pt electrode, TBAP, 0.1 mol l^{-1}; (a) ν(daad–CO); (b) ν(Re–CO). Baseline drift occurred during the experiment, giving rise to ill-defined isosbestic points in (a).

ligand. Similar results were obtained from OTTLE studies of related S- and O-containing heterocyclic quinones [26]. The ν(ReCO) bands shift to lower wavenumber by 5–8 cm^{-1} upon reduction, again indicative of an assemblage in which there is little communication between the donor radical anion and the organometallic acceptor.

Bands in the 1100–1750 cm^{-1} region in the resonance Raman spectrum of $\mathbf{2}^{\bullet -}$ at 457.9 and 514.5 nm excitation (Fig. 3) can again be assigned to the vibrations of $\mathbf{1}^{\bullet -}$. The observed enhancement of $\mathbf{1}^{\bullet -}$ bands and the absence of any change in intensity in the CO vibrational region are consistent with the assignment of the 620 nm band in the optical spectrum of $\mathbf{2}^{\bullet -}$ vide infra to a ligand-centred transition.

The parent spectrum is regenerated on reversal of the potential and isosbestic points in the UV–vis OTTLE spectra during the reduction of **2** are reproducible confirming that $\mathbf{2}^{\bullet -}$ is a stable radical anion.

Upon reduction, the MLCT band of **2** at 431 nm is bleached (Fig. 5). The electronic spectrum of $\mathbf{2}^{\bullet -}$ in the 400–1200 nm region, in fact, is remarkably similar to that of $\mathbf{1}^{\bullet -}$ (Table 2) which is supportive of the $\mathbf{1}^{\bullet -}$ assignment for the reduction of **2**.

3. Conclusion

Although the azaquinone ligand **1** reacts readily with $Re(CO)_n$ precursors, the thermodynamic end-point is always an insoluble product. However, the isolation of a

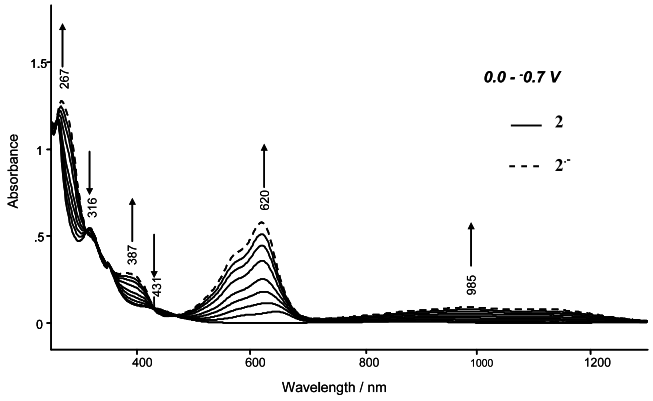

Fig. 5. UV–vis spectroelectrochemistry of **2** and $\mathbf{2}^{\bullet -}$ in CH_2Cl_2; Pt, TBAP, 0.1 mol l^{-1}.

soluble intermediate **2** has provided the first insight into the ground and excited states of a mononuclear $XRe(CO)_4(N)$ complex. UV–vis, Raman and IR spectroelectrochemistry show that **2** conforms to the standard orbital model deduced for $\{XRe(CO)_3(N–N)\}$ complexes; a ligand-based π* LUMO and a dπ HOMO on the Re(I) center. Compared to polypyridyl systems there is only weak dπ–π* coupling but this is sufficient to quench emission from the daad ligand [27].

4. Experimental

All reactions were carried out under nitrogen in dry solvents in oven-dried glassware. Cobaltocene, $ClRe(CO)_5$ and $Re_2(CO)_{10}$ were used as received (Strem). $BrRe(CO)_5$ [28], $FcRe(CO)_5$ [29] and **1** [30] were prepared by literature methods. Microanalyses were carried out by the Campbell Microanalytical Laboratory, University of Otago. NMR spectra were recorded on Varian VXR 500 or 300 MHz spectrometers. FTIR solution spectra were collected on a Perkin–Elmer Spectrum BX FTIR and UV–vis spectra on a Varian Cary 500 UV–vis–NIR. Resonance Raman spectra, generated with continuous wave excitation, were obtained using an air-cooled argon ion laser (Melles-Griot Omnichrome 543-MAP). Plasma emission lines were removed from the exciting beam using bandpass filters or a wavelength specific holographic laser bandpass filter (Kaiser Optical Systems Inc.). Typically, the laser output was adjusted to give 25 mW at the sample. An aperture-matched lens was used to focus scattered light through a narrow band line-rejection (notch) filter (Kaiser Optical Systems) and a quartz wedge (Spex) and onto the entrance slit of a spectrograph (Spex 750M). The collected light was dispersed in the horizontal plane by a 1800 grooves mm^{-1} holographic diffraction grating and detected by a liquid nitrogen cooled 1152-EUV CCD controlled by a ST-130 controller and CSMA 2.3b(v.2) software (Princeton Instruments). Spectra were analysed using GRAMS 5.0 (Galactic Industries). FAB mass spectra were recorded on a Kratos MS80RFA instrument with an Iontech ZN11NF atom gun and electrospray mass spectra on a VG Platform II spectrometer in a 1:1 v/v acetonitrile–water or methanol–water mobile phase (0.1 mM in compound). Electrochemical measurements were performed with a three-electrode cell using a computer controlled EG & G PAR 273A potentiostat/galvanostat at scan rates 0.05–10 V s^{-1}. A polished Pt disc electrode was employed; the reference was decamethylferrocene (CH_2Cl_2); the supporting electrolyte (0.1 M) was TBAH (CH_2Cl_2) and the sample $\sim 1 \times 10^{-3}$ M. The OTTLE cells used for Raman, IR and UV–vis spectroelectrochemistry were an in-house design [12].

4.1. Preparation of 2–4

$BrRe(CO)_5$ (406 mg, 1.00 mmol) was dissolved in dichloromethane (100 ml) and acetonitrile (1 ml). Me_3NO (75 mg, 1.00 mmol) was added and the solution was stirred for 2 h at 0 °C, then filtered through a silica pad and washed with dichloromethane. The solvent was removed in vacuo to obtain a white solid, which was dissolved in toluene (100 ml) and then **1** (105 mg, 0.50 mmol) added. The mixture was stirred at ambient temperature for 20 h and the solvent removed in vacuo to obtain an orange powder which was purified by chromatography. Elution on a silica gel column with dichloromethane removed the first minor orange fraction (tentatively identified as $[BrRe(CO)_4]_2$daad) then the second fraction was eluted with 1:1 ethyl acetate:-hexane to obtain **2** (90 mg, 15%) as an orange powder. Crystallisation from dichloromethane/hexane gave yellow plates suitable for X-ray crystallography. FAB *m/z* 588 M^+. ($C_{16}H_6BrN_2O_6Re$ requires: 588 M). $\nu(CH_2Cl_2$, cm^{-1}) 2115, 2016, 2004 (sh), 1943 (Re–CO), 1696 (CO). UV–vis (CH_2Cl_2; λ_{max}, nm): 316 ($\varepsilon = 5900$ M^{-1} cm^{-1}), 431 nm ($\varepsilon = 300$ M^{-1} cm^{-1}) $\delta_H(CDCl_3)$ 8.14 (1H, dd, $J = 5$ and 1 Hz, 7-H), 8.25 (1H, dd, $J = 6$ and 1 Hz, 3-H), 9.26 (1H, d, $J = 5$ Hz, 8-H), 9.63 (1H, d, $J = 1$ Hz, 5-H), 9.67 (1H, d, $J = 6$ Hz, 4-H), 9.96 (1H, d, $J = 1$ Hz, 1-H). $\delta_C(CDCl_3)$ 119.7, 122.6 (2 × CH), 137.5, 139.0, 149.9 (3 × 4 °C), 150.2, 156.3 (2 × CH), 156.4 (4 °C), 157.2, 161.3 (2 × CH), 180.0 (2 × CO), 185.5 (Re–CO). Elution of the third fraction with ethyl acetate gave **3** (132 mg, 68%) as an orange solid. (Found: C, 37.33; H, 1.58; N, 6.25; FAB *m/z*, 770 M^+. $C_{27}H_{12}BrN_4O_7Re \cdot 2CH_2Cl_2$ requires: C, 37.04; H, 1.72; N, 5.96). $\nu(CH_2Cl_2$, cm^{-1}) 2033, 1939, 1902 (Re–CO), 1695 (CO). UV–vis (CH_2Cl_2; λ_{max}, nm): 310 ($\varepsilon = 4500$ M^{-1} cm^{-1}), 395 ($\varepsilon = 400$ M^{-1} cm^{-1}). $\delta_H(CDCl_3)$ 8.07 (1H, d, $J = 5$ Hz, 7-H), 8.19 (1H, d, $J = 6$ Hz, 3-H), 9.22 (1H, d, $J = 5$ Hz, 8-H), 9.48 (1H, d, $J = 6$ Hz, 4-H), 9.61 (1H, s, 5-H), 9.70 (1H, s, 1-H). $\delta_C(CDCl_3)$ 119.2, 122.4 (2 × CH), 125.4, 128.0, 137.5, 138.8 (4 × 4 °C), 150.1, 154.8,

Table 3
Crystal data and structure refinement for **2**

Empirical formula	$C_{16}H_6N_2O_6BrRe$
Formula weight	588.34
Temperature (K)	163(2)
Crystal system	monoclinic
Space group	$P2_1/c$
a (Å)	14.985(7)
b (Å)	10.608(5)
c (Å)	10.554(5)
β (°)	93.456(5)
V (Å^3)	1674.8(13)
D_{calc} (g cm^{-3})	2.333
Z	4
μ(Mo–K$_\alpha$) (mm^{-1})	9.678
F(0 0 0)	1096
Crystal size (mm^3)	0.55 × 0.25 × 0.02
θ Range (°)	2.35–23.31
No. reflections collected	16 031
No. independent reflections	2397
R_{int}	0.0472
No. refined parameters	230
Goodness-of-fit on F^2	1.034
R_1 [$I > 2\sigma(I)$]	0.0269
wR_2 [a]	0.0778
Residuals (e Å^{-3})	1.622 and −1.052

[a] $R_1 = \Sigma||F_o|-|F_c||/\Sigma|F_o|$, $wR_2 = [\Sigma w(F_o^2-F_c^2)^2/\Sigma w(F_o^2)^2]^{1/2}$, $w = 1/[\sigma^2(F_o^2)+(0.0598P)^2]$ where $P = (F_o^2+2F_c^2)/3$.

157.0, 160.2 (4 × CH), 180.0, 180.2 (2 × CO), 195.0 (Re–CO).

1 (0.300 g, 1.43 mmol) was added under a nitrogen atmosphere to a suspension of $BrRe(CO)_5$ (0.579 g, 1.43 mmol) in THF:toluene (3:1, 140 ml). The greenish suspension was heated under reflux at 80 °C for 39 h. After ca. 15 h an orange precipitate was observed. The fine orange powder was filtered, washed with dichloromethane, diethyl ether and acetone and air dried to give **4** (0.720 g, 90%). (Found: C, 33.13; H, 1.33; N, 4.64. $(C_{15}H_6BrN_2O_5Re)_n \cdot CH_3COCH_3$ requires C, 32.91; H, 1.32; N, 4.87. ν(KBr, cm^{-1}) 2026, 1928, 1889 (Re–CO), 1691 (CO).

4.2. Preparation of $Cp_2Co^+2^{\bullet -}$

Cobaltocene (0.010 g, 5.3 × 10^{-2} mmol) was added to **2** (0.023 g, 3.9 × 10^{-2} mmol) dissolved in benzene. The suspension rapidly changed colour from orange to deep blue. After stirring for 30 min the mixture was filtered under a nitrogen atmosphere, rinsed with acetonitrile and dried in vacuo to obtain $\mathbf{Cp_2Co^+2^{\bullet -}}$ (0.18 g, 59%) as an extremely unstable blue/black powder which was soluble in acetonitrile and decomposed overnight. Electronic spectroscopic data was compatible with the UV–vis OTTLE results with the appearance of peaks at 593 and 976 nm.

4.3. Reactions with $ClRe(CO)_5$ and $FcRe(CO)_5$

$ClRe(CO)_5$ (0.172 g, 0.48 mmol) was dissolved in hexane (50 ml) and 1 (0.200 g, 0.95 mmol) was added. The green suspension was stirred under reflux at 60 °C for 6 h, during which time an orange precipitate was observed. The insoluble orange powder was filtered and washed with dichloromethane and acetone to obtain $[ClRe(CO)_3(daad)]_n$ (0.049 g, 10%). Found: C, 34.97; H, 1.13; N, 5.28; $C_{15}H_6ClN_2O_5Re$ requires: C, 34.92; H, 1.17; N, 5.43. ν(KBr, cm^{-1}): 2027, 1934, 1883 (M–CO), 1692 (daad CO). The filtrate was concentrated in vacuo to obtain an orange solid which was purified by silica gel plate chromatography. Elution with dichloromethane:-diethyl ether:hexane (10:4:1) gave $ClRe(CO)_3(daad)_2$ (0.155 g, 45%) as an orange solid ($R_f = 0.15$). $\nu(CH_2Cl_2$, cm^{-1}): 2032, 1936, 1899 (M–CO), 1695 (daad CO). $\delta_H(CDCl_3)$ 8.06 (1H, d, $J = 5$ Hz, 6-H), 8.20 (1H, d, $J = 6$ Hz, 2H), 9.22 (1H, d, $J = 5$ Hz, 5H), 9.44 (1H, d, $J = 6$ Hz, 3-H), 9.60 (1H, s, 4-H), 9.69 (1H, s, 1-H). From a similar reaction in THF:toluene (3:1) an orange precipitate was observed after 15 h. The fine orange powder was filtered, washed with dichloromethane, diethyl ether and acetone and air dried to give $[ClRe(CO)_3(daad)]_n$ (0.710 g, 96%). Similar reactions with $FcRe(CO)_5$ always gave an insoluble brown precipitate with no TLC or spectroscopic evidence for intermediates.

5. X-ray structural analysis

Crystal data for **2** are given in Table 3. **2** was crystallised from dichloromethane/hexane and yellow plates was used for data collection. Data were collected on a Bruker SMART CCD diffractometer processed using SMART and SAINT [31] and empirical absorption corrections applied using SADABS [31]. The structure was solved using SHELXS-97 [32] and refined by full matrix least squares on F^2 using SHELXL-97 [32] and TITAN2000 [33]. All non-hydrogen atoms were assigned anisotropic temperature factors, with hydrogen atoms included in calculated positions.

6. Supplementary material

Crystallographic data for the structural analysis have been deposited with the Cambridge Crystallographic Data Centre, CCDC no. 204411 for compound **2**. Copies of this information may be obtained free of charge from The Director, CCDC, 12 Union Road, Cambridge CB2 1EZ, UK (Fax: +44-1223-336033; e-mail: deposit@ccdc.cam.ac.uk or www: http://www.ccdc.cam.ac.uk).

Acknowledgements

We thank Prof. W.T. (University of Canterbury) for the collection of X-ray data and Dr A.L. and Prof. P.H. for measuring the esr spectrum of $\mathbf{2}^{\bullet -}$. Financial support came from the Marsden Fund, Royal Society of NZ, and the University of Otago.

References

[1] (a) D.W. Bruce, D. Ohare (Eds.), Inorganic Materials, Wiley, Chichester, England, 1992;
(b) J.M. Lehn, Supramolecular Chemistry, VCH, Weinheim, 1995.
[2] (a) V. Balzani, F. Scandola (Eds.), Supramolecular Photochemistry, Horwood, Chichester, England, 1991;
(b) M. Ward, Chem. Ind. (1997) 640.
[3] (a) A.P. De Silva, H.Q.N. Gunaratne, T. Gunnlaugsson, A.J.M. Huxley, C.P. McCoy, J.T. Rademacher, T.E. Rice, Chem. Rev. 97 (1997) 1515;
(b) J.-P. Desvaergne, A.W. Czarnik (Eds.), Chemosensor of Ion and Molecule Recognition, Kluwer, Dordrecht, 1997;
(c) B. Valeur, Topics in fluorescence spectroscopy, in: J.R. Lakowicz (Ed.), Probe Design and Sensing, vol. 4, Plenum, New York, 1994, p. 21.
[4] (a) G. Che, E.R. Fisher, C.R. Martin, Nature 393 (1998) 346–349;
(b) D. Campbell, B.R. Herr, J.C. Hulteen, R.P. Van Duyne, C.A. Mirkin, J. Am. Chem. Soc. 118 (1996) 10211.
[5] (a) R.V. Slone, K.D. Beckstein, S. Belanger, J.T. Hupp, I.A.A. Gunzei, A.L. Rheingold, Coordin. Chem. Rev. 171 (1998) 221;
(b) V. Grosshenny, A. Harriman, M. Hissler, R. Ziessel, Platinum Metal Rev. 40 (1996) 26.
[6] M.S. Wrighton, L. Pdungsap, D.L. Morse, J. Phys. Chem. 79 (1975) 66.
[7] (a) P.J. Stang, B. Olenyuk, Acc. Chem. Res. 30 (1997) 502;
(b) B. Olenyuk, A. Fechtenkotter, P.J. Stang, J. Chem. Soc. Dalton Trans. (1998) 1707.
[8] (a) S.M. Woessner, J.B. Helms, Y. Shen, B.P. Sullivan, Inorg. Chem. 37 (1998) 5406;
(b) K.D. Beckstein, J.T. Hupp, C.L. Stern, J. Am. Chem. Soc. 120 (1998) 12982 (references therein).
[9] P.J. Stang, B. Olenyuk, Angew. Chemie Int. Ed. 35 (1996) 732.
[10] V. Rajendran, B. Manimaran, F.-Y. Lee, G.-H. Lee, S.-M. Ping, C.M. Wang, K.-L. Lu, Inorg. Chem. 39 (2000) 2016.
[11] (a) J.R. Schoonover, C.A. Bignozzi, T.J. Meyer, Coordin. Chem. Rev. 165 (1997) 239;
(b) J.R. Schoonover, G.F. Strouse, Chem. Rev. 98 (1998) 1335.
[12] M.R. Waterland, T.J. Simpson, K.C. Gordon, A.K. Burrell, J. Chem. Soc. Dalton Trans. (1998) 185.
[13] R.W. Balk, D.J. Stufkens, A. Oskam, J. Chem. Soc. Dalton Trans. (1981) 1124.
[14] O. Briel, K. Sünkel, I. Krossing, H. Nöth, E. Schmälzlin, K. Meerholz, C. Bräuchle, W. Beck, Eur. J. Inorg. Chem. (1999) 483.
[15] J.L. Morgan, A. Flood, K.C. Gordon, H.G. Kjaergaard, B.H. Robinson, J. Simpson, Aus. J. Chem., in press.
[16] (a) W. Werner, U. Gräfe, W. Ihn, D. Tresselt, S. Winter, E. Paulus, Tetrahedron 53 (1997) 109;
(b) T. Billert, R. Beckert, P. Fehling, M. Döring, H. Görls, Tetrahedron 53 (1997) 5455;
(c) A. Opitz, E. Roemer, W. Haas, H. Görls, W. Werner, U. Gräfe, Tetrahedron 56 (2000) 5147.
[17] (a) W. Tikkanen, W.C. Kaska, S. Moya, T. Layman, R. Kane, C. Kruger, Inorg. Chim. Acta 76 (1983) L29;
(b) E.W. Abel, V.S. Dimitrov, N.J. Long, K.G. Orrell, A.G. Osborne, H.M. Pain, V. Sik, M.J. Hursthouse, M.A. Mazid, J. Chem. Soc. Dalton Trans. (1993) 597;
(c) S.A. Moya, R. Schmidt, R. Pastene, R. Sartori, U. Muller, G. Frenzen, Organometallics 15 (1996) 3463;
(d) A. Gelling, K.G. Orrell, A.G. Osborne, V. Sik, M.B. Hursthouse, S.J. Coles, J. Chem. Soc. Dalton Trans. (1996) 203.
[18] M.C. Couldwell, J. Simpson, J. Cryst. Struct. Comm. 6 (1977) 1.
[19] Similar results were obtained with reactions of $XRe(CO)_5$ (X = Cl, Fc) with 2,6-diazaanthracene (daa).
[20] (a) Y.L. Lee, J.R. Kirchoff, R.M. Berger, D. Gosztola, J. Chem. Soc. Dalton Trans. (1995) 3677;
(b) T.J. Simpson, K.C. Gordon, Inorg. Chem. 34 (1995) 6323;
(c) S.B. Jimenez-Pulido, M. Sieger, A. Knodler, O. Heilmann, M. Wanner, B. Schwederski, J. Fiedler, M.N. Moreno-Carretero, W. Kaim, Inorg. Chim. Acta 325 (2001) 65;
(d) F. Hornung, M. Wanner, K.W. Klinkhammer, W. Kaim, J.Z. Fiedler, Anorg. Allg. Chem. 627 (2001) 2430;
(e) T. Scheiring, J. Fiedler, W. Kaim, Organometallics 20 (2001) 1437;
(f) H. Hartmann, T. Scheiring, J. Fiedler, W. Kaim, J. Organomet. Chem. 604 (2000) 267;
(g) A. Klein, V. Vogler, W. Kaim, Organometallics 15 (1996) 236 (references therein).
[21] J.R. Schoonover, P. Chen, W.D. Bates, R.B. Dyer, T.J. Meyer, Inorg. Chem. 33 (1994) 793.
[22] A.B.P. Lever, E.S. Dodsworth, Inorganic Electronic Structure and Spectroscopy, vol. 2, Wiley, NY, 1999.
[23] S.E. Page, A. Flood, K.C. Gordon, J. Chem. Soc. Dalton Trans. (2002) 1180.
[24] Similar g values for $\mathbf{1}^{\bullet -}$ and $\mathbf{2}^{\bullet -}$ were observed in their esr spectra, good evidence that the SOMO of $\mathbf{2}^{\bullet -}$ has little rhenium character. However, for both species the spectra unexpectedly show no hyperfine coupling [15] and a detailed analysis was not possible.
[25] B.R. Clark, D.H. Evans, J. Electroanal. Chem. 69 (1976) 181.
[26] M. Buschel, C. Stadler, C. Lambert, M. Beck, J. Daub, J. Electroanal. Chem. 484 (2000) 24.
[27] Both **2** and $\mathbf{2}^{\bullet -}$ were found to be non-emissive at room temperature in CH_2Cl_2.
[28] S.P. Schmidt, W.C. Trogler, F. Basolo, Inorg. Syn. 23 (1985) 41.
[29] T.M. Miller, K.J. Ahmed, M.S. Wrighton, Inorg. Chem. 28 (1989) 2347.
[30] V. Bollit, C. Mioskowski, S.P. Reddy, J.R. Falck, Synthesis (1988) 388.
[31] (a) SMART (Control) and SAINT (Integration) software, Bruker, AXS, Madison WI, 1994.;
(b) SADABS (correction for area detector data), Bruker AXS, Madison WI, 1997.
[32] (a) G.M. Sheldrick, SHELXS-96. A Program for the Solution of Crystal Structures from Diffraction Data, University of Göttingen, Germany, 1996;
(b) G.M. Sheldrick, SHELXL-97. A Program for the Refinement Crystal Structures, University of Göttingen, Germany, 1997.
[33] K.A. Hunter, J. Simpson, TITAN2000. A Molecular Graphics Program to Aid Structure Solution and Refinement with the SHELX Suite of Programs, University of Otago, New Zealand, 1999.